

## Supporting Information

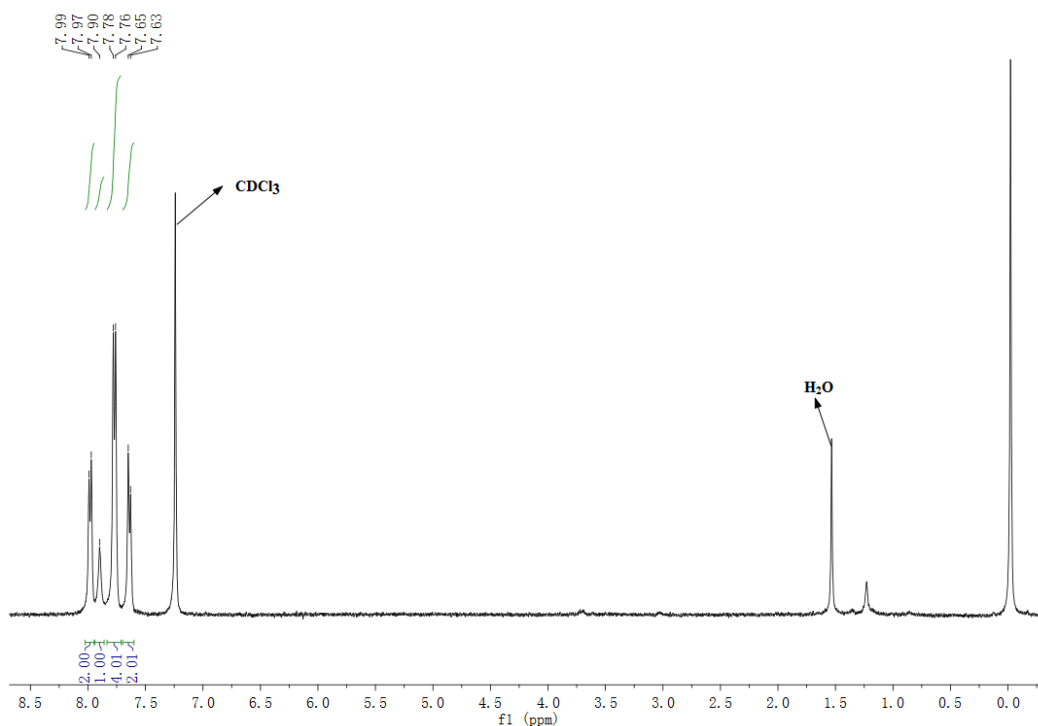
# Highly Efficient Single Emissive Layer Orange and Two-Element White Organic Light-Emitting Diodes by Solution Prozesse

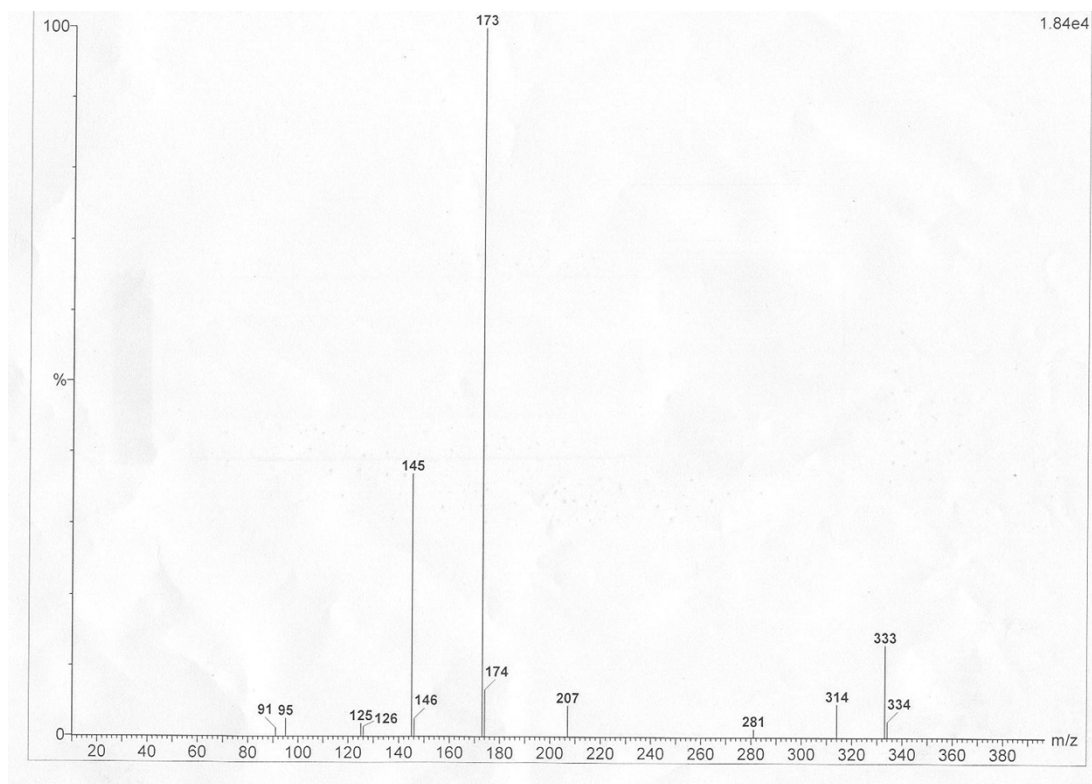
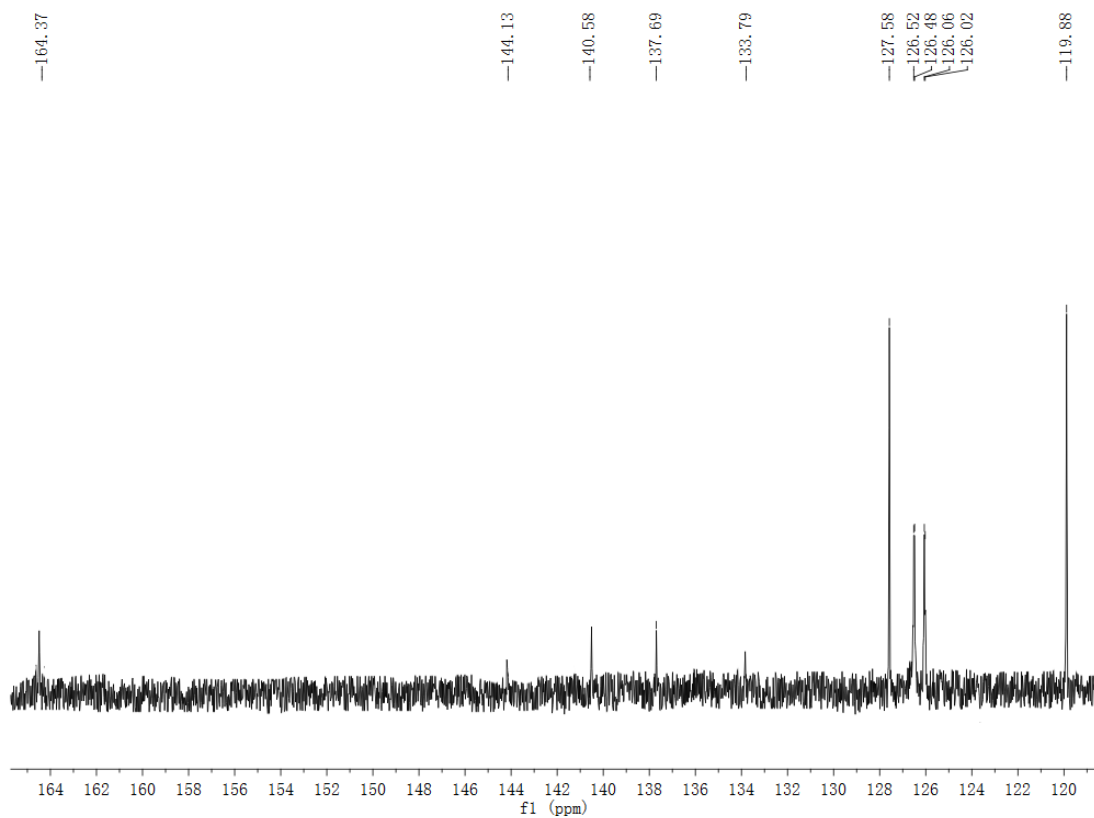
Jinshan Wang, Xinjun Xu,\* Yuan Tian, Chuang Yao, Lidong Li\*

State Key Lab for Advanced Metals and Materials, School of Materials Science and Engineering, University of Science and Technology Beijing, Beijing 100083, P. R. China.

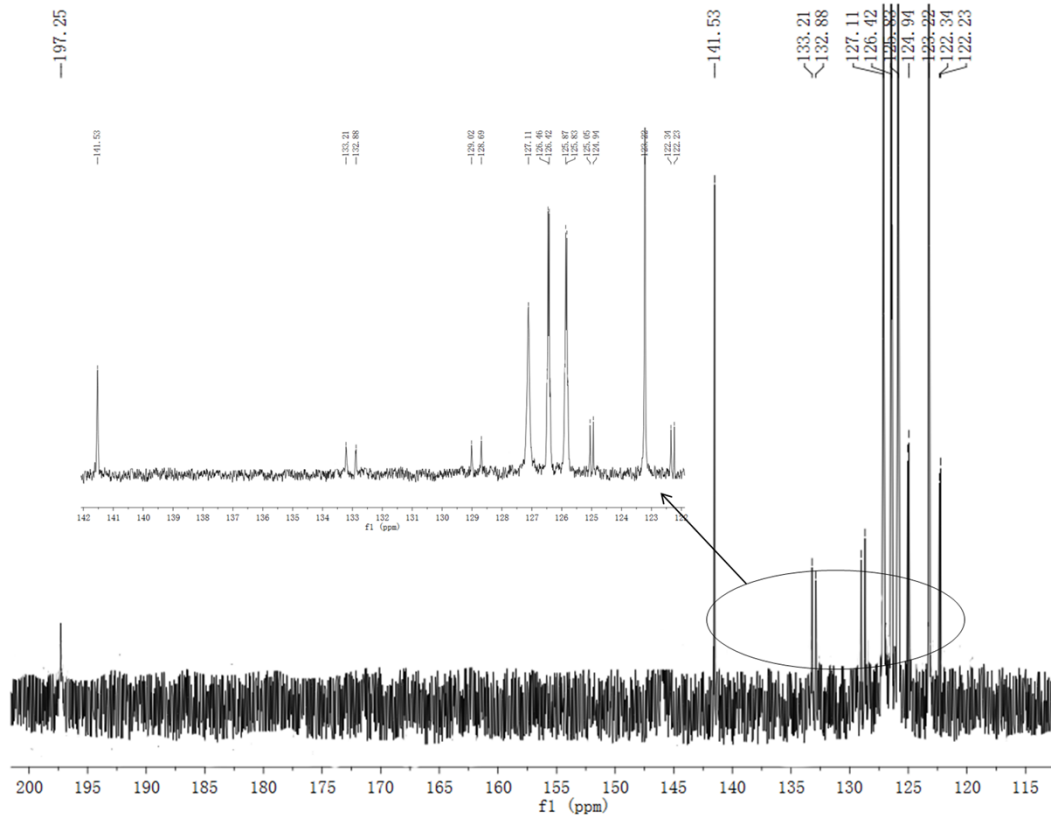
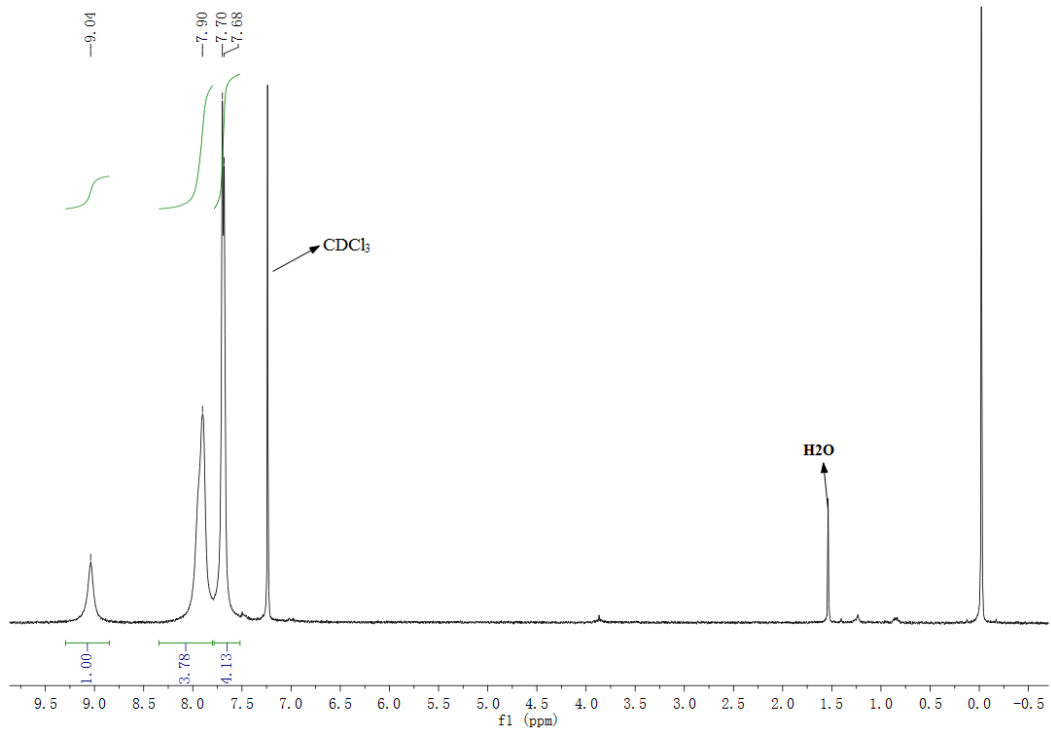
E-Mail: lidong@mater.ustb.edu.cn; xuxj@mater.ustb.edu.cn

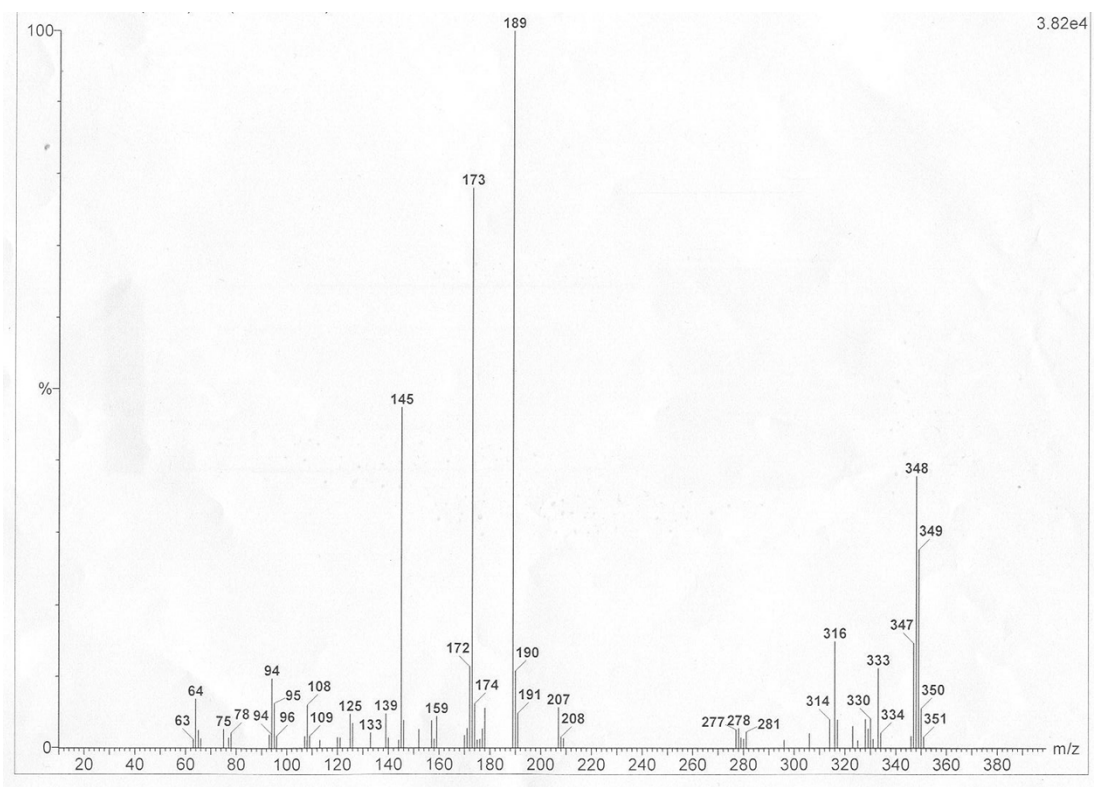
$^1\text{H}$ NMR,  $^{13}\text{C}$ NMR and MS(EI) of **1**:



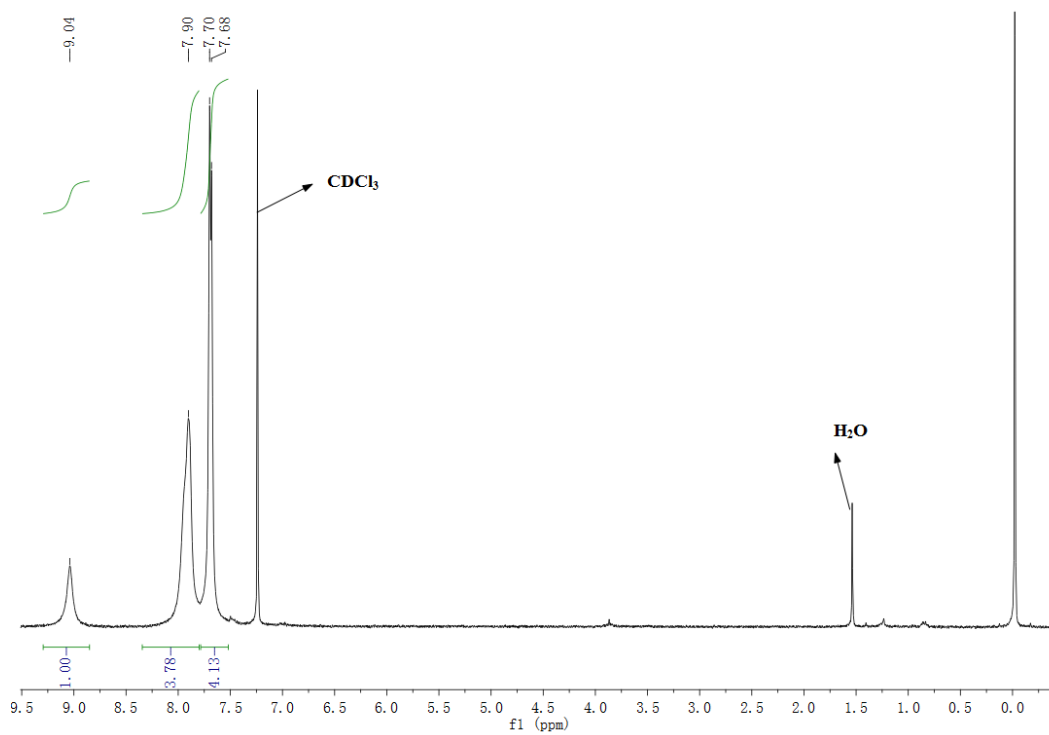


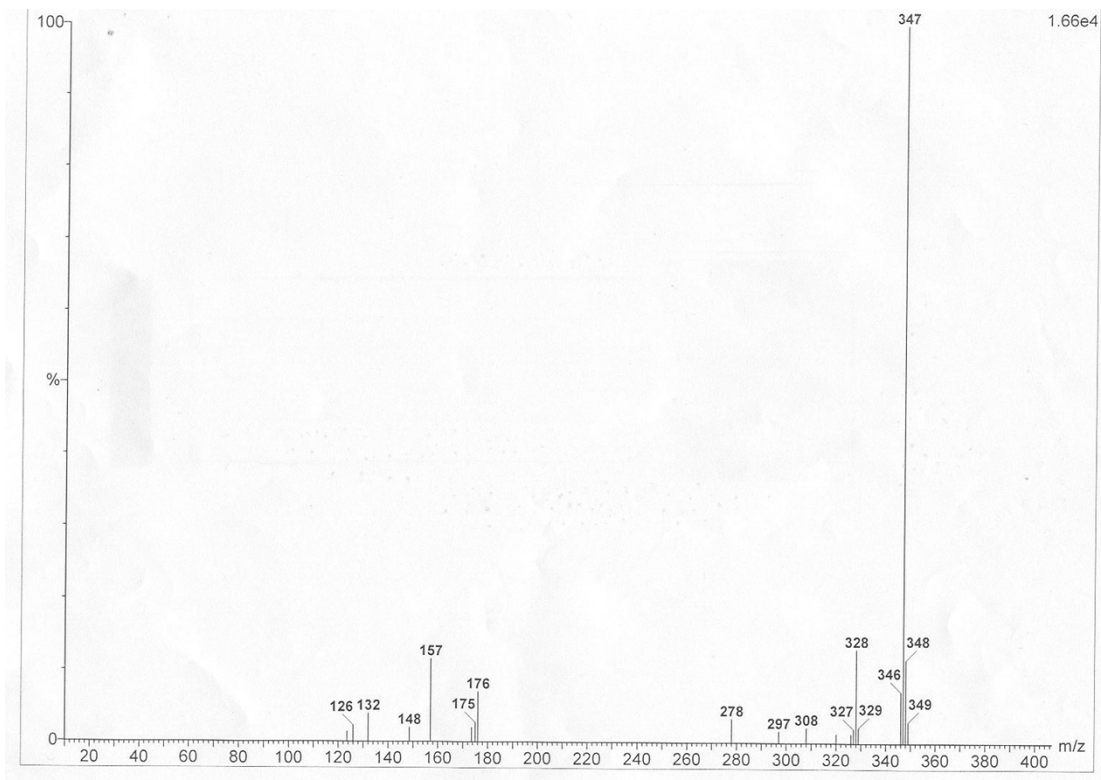
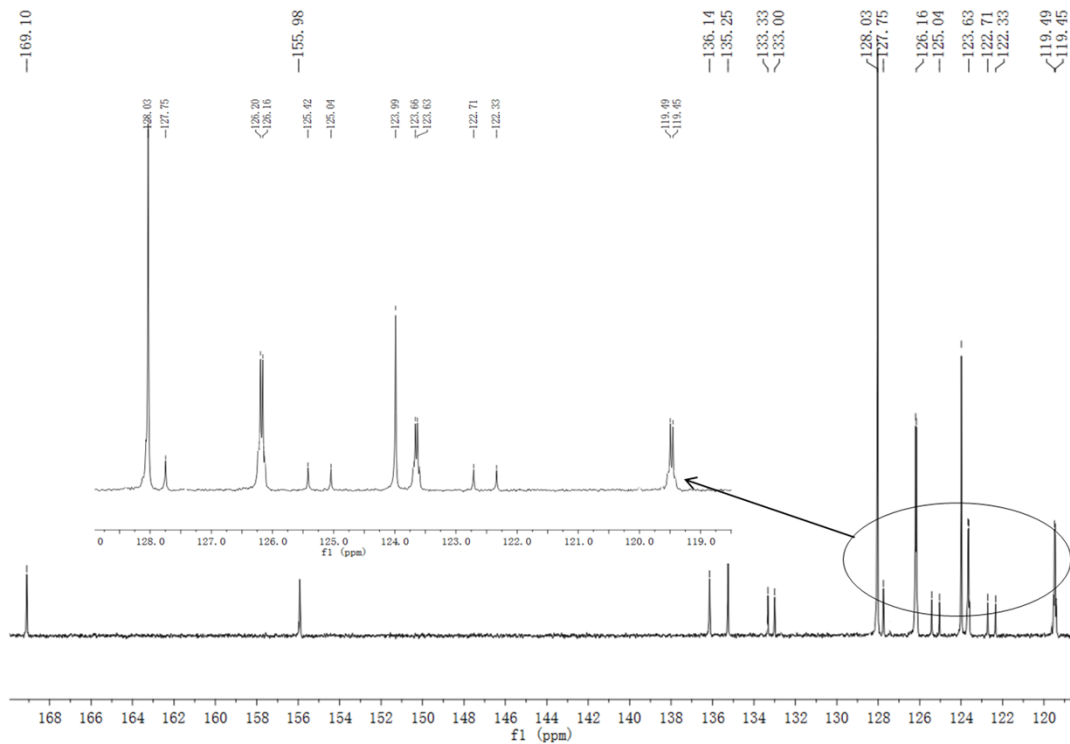
<sup>1</sup>H NMR, <sup>13</sup>C NMR and MS(EI) of 2:



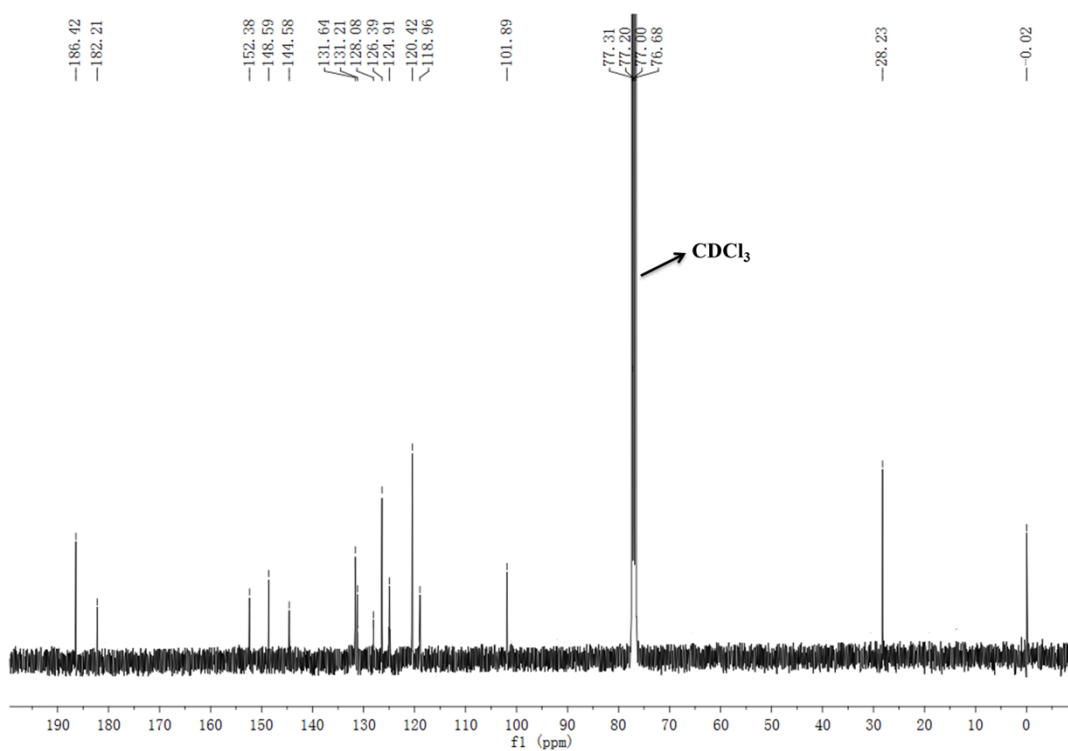
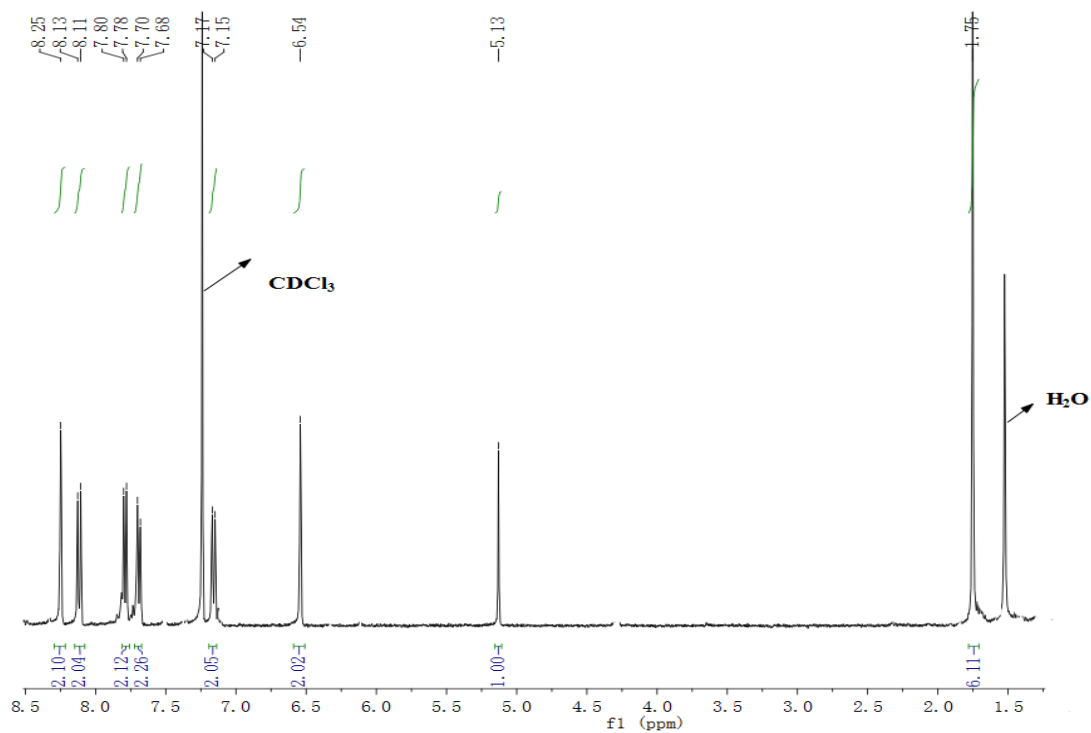


$^1\text{H}$ NMR,  $^{13}\text{C}$ NMR and MS(EI) of **3**:





$^1\text{H}$ NMR,  $^{13}\text{C}$ NMR and MALDI-TOF mass spectra of  $(\text{CF}_3\text{BT-CF}_3\text{P})_2\text{Ir}(\text{acac})$ :



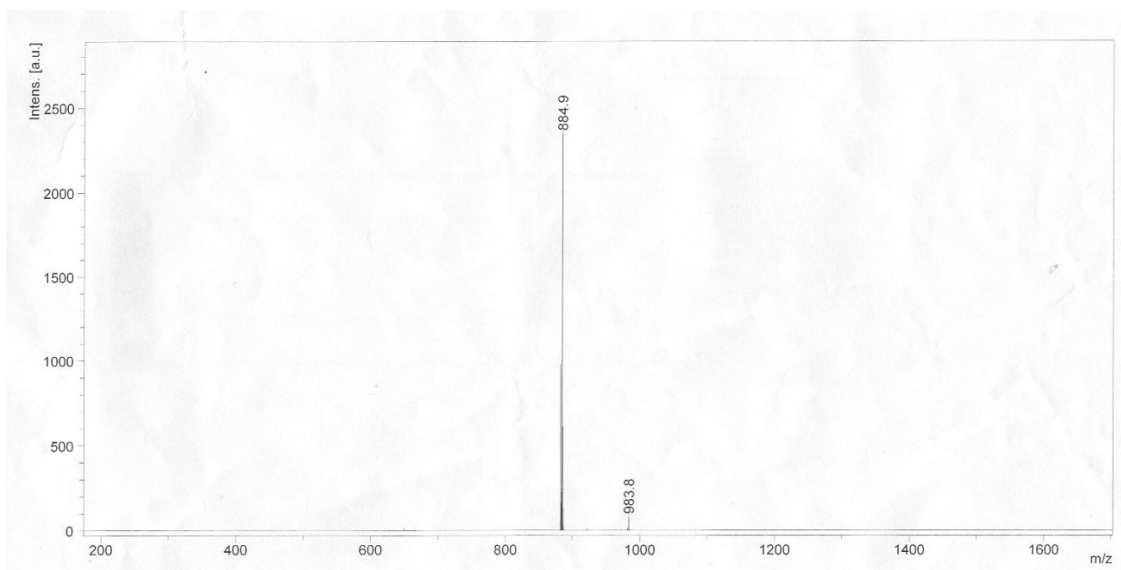


**Fig. S1** The NMR spectra and mass spectra (MS) of all compounds.

**Table S1.** The photoluminescent quantum yields of  $(\text{CF}_3\text{BT-CF}_3\text{P})_2\text{Ir}(\text{acac})$  under different doping concentrations in solid states.

Doping concentration <sup>a</sup>	20:1	10:1	5:1	0:1
$\Phi_p$ (%)	67	62	42	1.8

<sup>a</sup> The w/w concentration of PVK: iridium complex.

**Table S2.** Frontier molecular orbital (FMO) energies ( $E$ , eV) and compositions (%) of  $(\text{CF}_3\text{BT-CF}_3\text{P})_2\text{Ir}(\text{acac})$  in the lowest-triplet excited state in the gas phase under vacuum.

FMO <sup>a</sup>	$E$ (eV)	MO composition (%) <sup>b</sup>				Assignment
		Ir	PBT-1	PBT-2	acac	
L	-2.73	4	94	1	1	$\pi^*(\text{PBT-1})$
H	-5.70	40	33	21	6	$d(\text{Ir})+\pi(\text{PBT-1}+\text{PBT-2})$
H-1	-5.95	30	8	7	55	$d(\text{Ir})+\pi(\text{acac})$
H-2	-6.35	12	52	13	23	$d(\text{Ir})+\pi(\text{PBT-1}+\text{PBT-2}+\text{acac})$

<sup>a</sup> H=HOMO, L=LUMO, H-1=HOMO-1, H-2=HOMO-2. <sup>b</sup> PBT=2-phenyl benzothiazole.

**Table S3.** Calculated orbital transition analyses based on the geometry optimization of the lowest-lying triplet state.

State	Configuration <sup>a</sup>	Assignment <sup>b</sup>	MLCT <sup>c</sup> (%)
S <sub>0</sub> -T <sub>1</sub>	H→L(22%)	d(Ir)+π(PBT-1+ PBT-2) →π*( PBT-1)/MLCT/LLCT/IL	23.5
	H-1→L(55%)	d(Ir)+π(acac) →π*( PBT-1)/MLCT/LLCT	
	H-2→L(16%)	d(Ir)+π(PBT-1+PBT-2+acac)→π*(PBT-1)/MLCT/LLCT/IL	

<sup>a</sup> H=HOMO, L=LUMO, H-1=HOMO-1, H-2=HOMO-2. <sup>b</sup> PBT=2-phenyl benzothiazole. MLCT, LLCT and IL denote metal-to-ligand charge transfer, ligand-to-ligand charge transfer and intraligand, respectively. <sup>c</sup>  $MLCT(\%) = \sum_{m,n} [C_I(m \rightarrow n)]^2 (\% (M)_m - \% (M)_n)$ ,<sup>[1]</sup> where  $\% (M)_{m,n}$  is

the molecular orbital (MO) composition contributed from the metal to the orbital involved in the transition model of MO(m)→MO(n),  $C_I(m \rightarrow n)$  is the corresponding coefficients of the I-th eigenvector of the configuration interaction (CI) matrix, so  $[C_I(m \rightarrow n)]^2$  is the contribution of this electron transition model to the S<sub>0</sub>→T<sub>1</sub> transition.



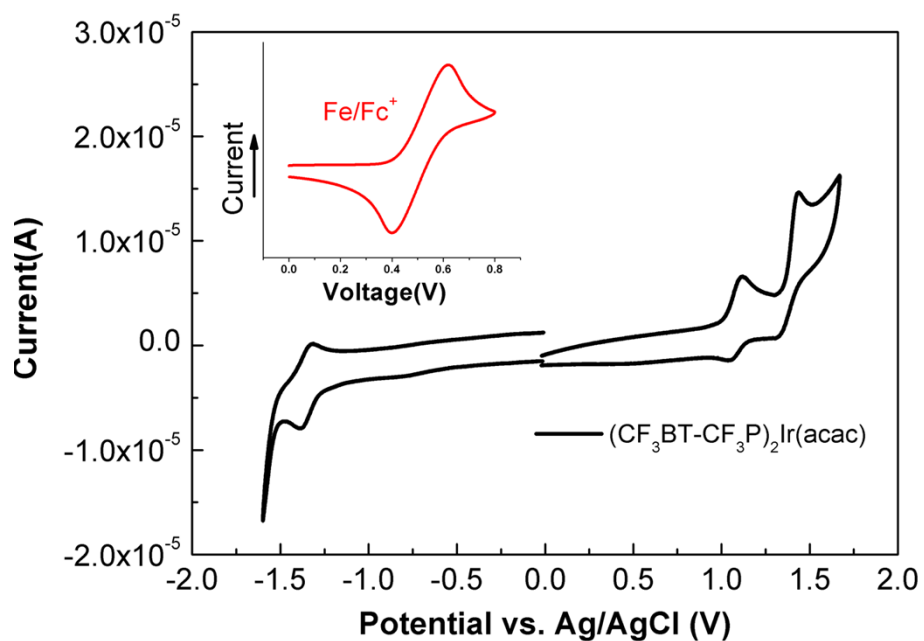


**Fig. S2** Cyclic voltammogram of  $(\text{CF}_3\text{BT-CF}_3\text{P})_2\text{Ir}(\text{acac})$  in  $\text{CH}_2\text{Cl}_2$  with 0.1 M  $\text{Bu}_4\text{NPF}_6$  as the electrolyte at a potential scan rate of  $30 \text{ mV s}^{-1}$ . The inset shows the redox curve of ferrocene. The first oxidation peak was used to calculate the HOMO level of  $(\text{CF}_3\text{BT-CF}_3\text{P})_2\text{Ir}(\text{acac})$ .

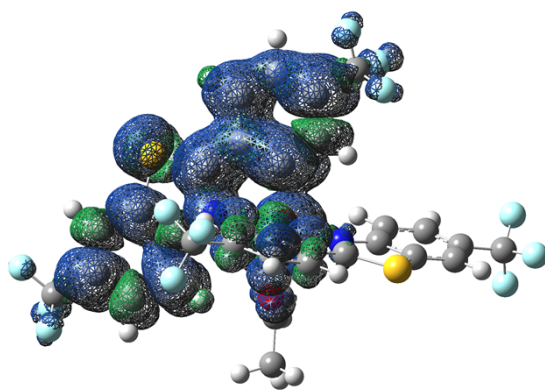


**Fig. S3** The spin density of the triplet electronic configuration of  $(\text{CF}_3\text{BT-CF}_3\text{P})_2\text{Ir}(\text{acac})$  (the blue balloons indicate regions where the spin density is positive and the green balloons the regions where the spin density is negative).

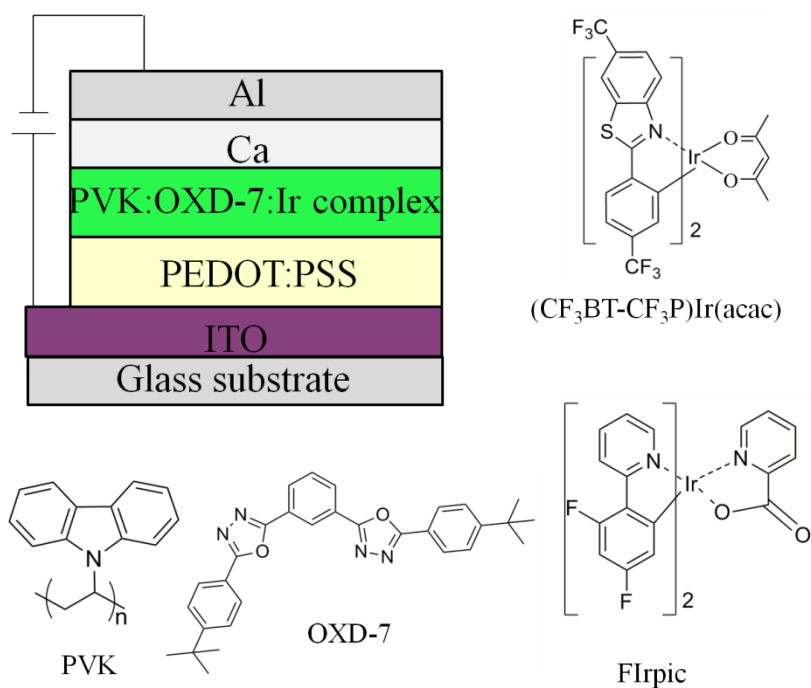


**Fig. S4** The device configuration of monochromatic orange OLEDs and two–element WOLEDs together with the molecular structures of compounds used in these devices.

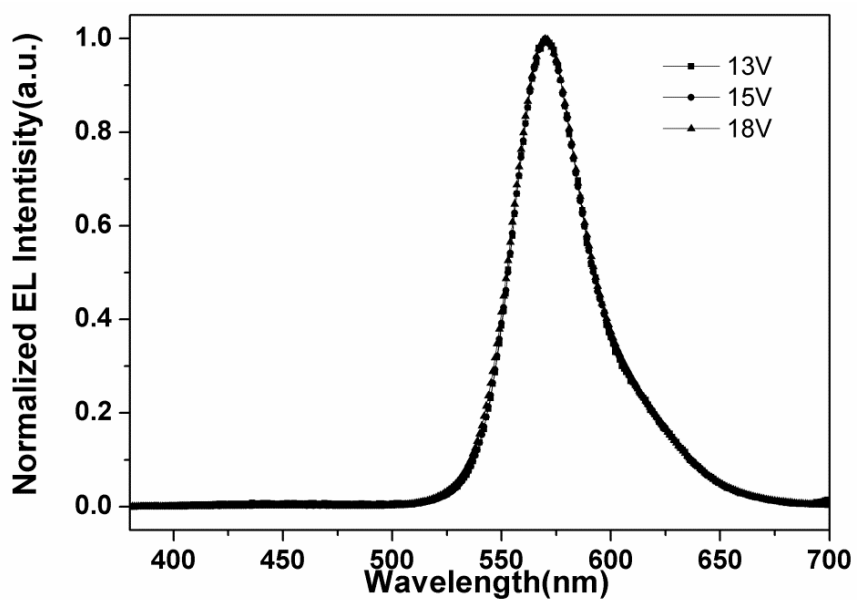


**Fig. S5** The EL spectra of device A under various driving voltages.

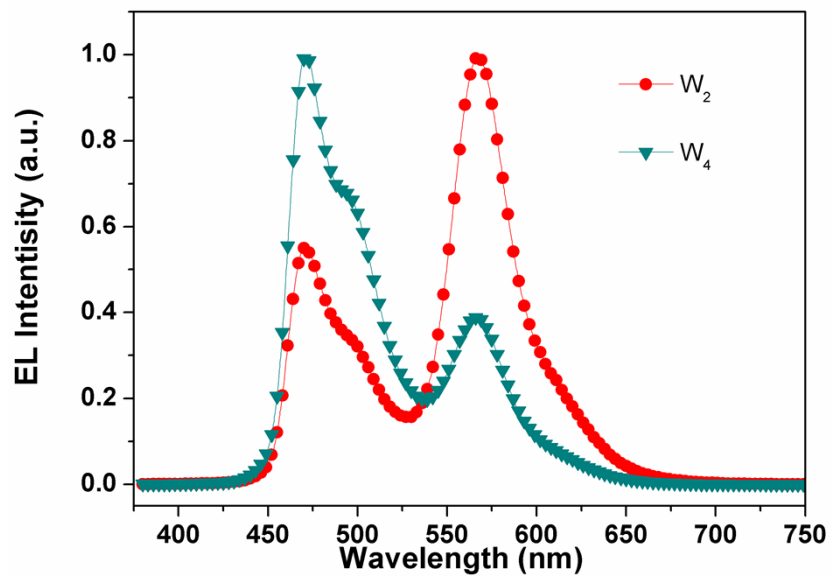


Fig. S6 The EL spectrum of  $W_2$  and  $W_4$  at 12 V.

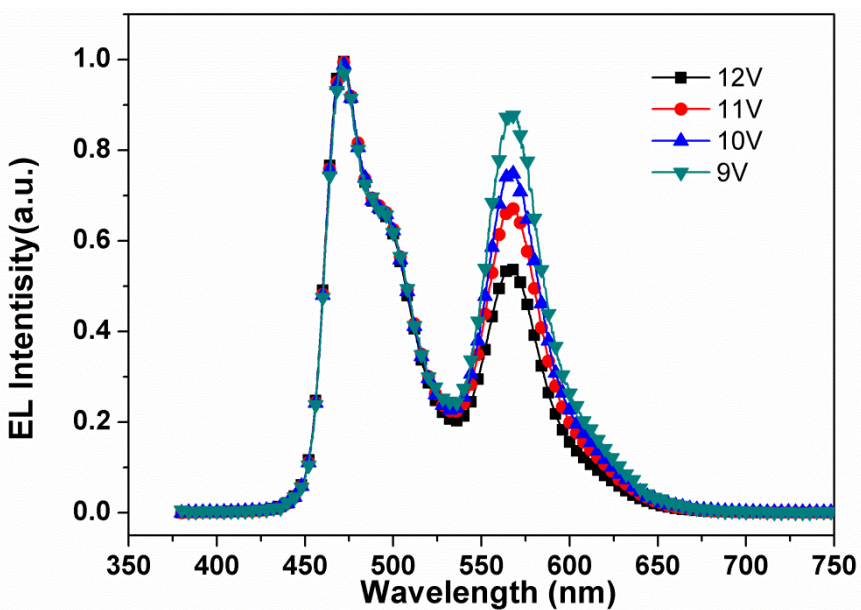


Fig. S7 The EL spectra of device  $W_3$  under various driving voltages.

## References

- 1 S. I. Gorelsky and A. B. P. Lever, *Can. J. Anal. Sci. Spectr.*, 2003, **48**, 93.